· Review · Advances in Polar Science
doi: 10.13679/j.advps.2021.0038 June 2022 Vol. 33 No. 2: 123-134

The evaluation of biological productivity by triple isotope composition of oxygen trapped in ice-core bubbles and dissolved in ocean: a review

ZHOU Yaqian[1], PANG Hongxi[1*], HU Huanting[2], YANG Guang[1] & HOU Shugui[2]

[1] Key Laboratory of Coast and Island Development of Ministry of Education, School of Geography and Ocean Science, Nanjing University, Nanjing 210023, China;
[2] Institute of Oceanography, Shanghai Jiao Tong University, Shanghai 200240, China

Received 21 July 2021; accepted 21 October 2021; published online 21 November 2021

Abstract The ^{17}O anomaly of oxygen ($\Delta^{17}O$, calculated from $\delta^{17}O$ and $\delta^{18}O$) trapped in ice-core bubbles and dissolved in ocean has been respectively used to evaluate the past biosphere productivity at a global scale and gross oxygen production (GOP) in the mixed layer (ML) of ocean. Compared to traditional methods in GOP estimation, triple oxygen isotope (TOI) method provides estimates that ignore incubation bottle effects and calculates GOP on larger spatial and temporal scales. Calculated from TOI of O_2 trapped in ice-core bubbles, the averaged global biological productivities in past glacial periods were about 0.83–0.94 of the present, and the longest time record reached 400 ka BP (thousand years before the present). TOI-derived GOP estimation has also been widely applied in open oceans and coastal oceans, with emphasis on the ML. Although the TOI method has been widely used in aquatic ecosystems, TOI-based GOP is assumed to be constant at a steady state, and the influence of physical transports below the ML is neglected. The TOI method applied to evaluate past total biospheric productivity is limited by rare samples as well as uncertainties related to O_2 consumption mechanisms and terrestrial biosphere's hydrological processes. Future studies should take into account the physical transports below the ML and apply the TOI method in deep ocean. In addition, study on the complex land biosphere mechanisms by triple isotope composition of O_2 trapped in ice-core bubbles needs to be strengthened.

Keywords **triple oxygen isotope, ice-core bubbles, dissolved oxygen in ocean, biological productivity**

Citation: Zhou Y Q, Pang H X, Hu H T, et al. The evaluation of biological productivity by triple isotope composition of oxygen trapped in ice-core bubbles and dissolved in ocean: a review. Adv Polar Sci, 2022, 33(2): 123-134, doi: 10.13679/j.advps.2021.0038

1 Introduction

Biospheric productivity plays a vital role in controlling the concentration of carbon dioxide in the atmosphere, which influences the global carbon cycle, and subsequently causes global climate change. Both terrestrial and oceanic biological production are primary mechanisms for global oxygen production and carbon uptake. Because the oceans sink around 30% of anthropogenic carbon dioxide emission (IPCC, 2014), evaluating marine photosynthetic productivity is key to understand the global carbon cycle at present and predict the response of carbon cycle to climate forcing in the future.

There are several traditional methods used to assess the biosphere productivity. For instance, $H_2{}^{18}O$ spike incubation (Grande et al., 1989) used labeled $H_2{}^{18}O$ to estimate GOP based on the evolution of $^{18}O_2$. Because of the large enrichments in ^{18}O, this method is easier than triple oxygen isotope (TOI) method in tracing natural variations and is less affected by photosynthetic

* Corresponding author, ORCID: 0000-0003-3990-6566, E-mail: hxpang@nju.edu.cn

fractionation (Bender et al., 1987; Stanley and Howard, 2013). However, it is susceptible to sampling, manipulation and containment effects, and it alone cannot characterize respiratory mechanisms in aquatic O_2 uptake (Luz et al., 2002; Manning et al., 2007a; Tobias et al., 2007; Staehr et al., 2012; Hotchkiss and Hall, 2014). Light or dark incubation (Harris et al., 1989) experiment is an O_2-based in vitro approach that is convenient for sampling and is widely applied to assess oceanic production, but its assumption of equal dark and light O_2 uptake rates will bring about large errors (Manning et al., 2007a). The ^{14}C in vitro incubation (Nielsen, 1952) is one of the oldest and most widely used method to quantify primary productivity (Bender et al., 1987; Manning et al., 2017b). However, uncertainties of the ^{14}C method remain regarding to whether it reflects the natural environment ("bottle effect") (Peterson, 1980; Harrison and Harris, 1986) and to its near-instantaneous measurements (6–24 h) (Marra, 2007), as well as to the ambiguity between net community production and gross primary production (Bender et al., 1999). Remote sensing data and satellite algorithms (Behrenfeld and Falkowski, 1997) can estimate marine photosynthetic O_2 production globally with high spatial and temporal resolution (Juranek and Quay, 2013), but it is lacking in field data for validation, and is confined to measurement of primary production in the surface layer. Fast Repetition Rate Fluorometry (FRRF) (Suggett et al., 2001; Moore et al., 2003) enables high-frequency real-time calculation of primary production, but the assumptions of the FRRF still contain large uncertainties (Fujiki et al., 2008). Having understood the strengths and shortcomings of traditional methods, here we review the newly-developed TOI approach.

Over the past two decades, the triple isotope composition of oxygen (^{16}O, ^{17}O and ^{18}O) trapped in ice-core bubbles and dissolved oxygen in ocean have been respectively used to evaluate the past global biosphere productivity (including both terrestrial and oceanic biosphere) (Luz et al., 1999; Blunier et al., 2002, 2012) and gross oxygen production (GOP) in the mixed layer (ML) of ocean (Luz and Barkan, 2000; Sarma et al., 2005; Juranek and Quay, 2010; Prokopenko et al., 2011; Bender et al., 2016). Paleo-atmospheric O_2 and dissolved O_2 bear the isotopic fractionation from both stratosphere and biosphere, in which oxygen isotopes are fractionated in a mass-independent way and a mass-dependent way, respectively. By measuring $\Delta^{17}O$ (defined in section 2.1, equation (2)) in marine dissolved oxygen and paleo O_2 occluded in ice-core bubbles, accompanied with air-sea gas transfer rates and atmospheric CO_2 concentration, one can determine the marine photosynthetically produced oxygen and the global biological productivity in the past. TOI method has several advantages in assessing biospheric productivity. First, at a steady state, it reflects community productivity over the residence time (1–3 weeks) of dissolved O_2 (Reuer et al., 2007; Li et al., 2019), improving the temporal scale of primary productivity assessment. Second, the TOI method can be used in oceanic zones over a wide range of longitudes and latitudes, improving the spatial scale of marine productivity observations (Juranek and Quay, 2013). Also, TOI method can be applied in fresh water ecosystems (Jurikova et al. 2016; Howard et al. 2020). Finally, the calculation of $\Delta^{17}O$ is independent on respiration (Quay et al., 1993; Hendricks et al., 2005), which diminishes errors resulted from complex respiratory mechanisms. Although TOI method also has shortcomings, such as uncertainties from analytical errors, gas exchange coefficients (k), and gas separation procedures, it is still prospective and worthy of further study in terms of its wide application in assessing marine and global biological productivity. With this in mind, we hope to provide a review of how this approach is applied to evaluation of biological productivity and issues that can be paid attention to in the future.

2 Principles

2.1 Fractionation mechanisms and calculation of $\Delta^{17}O$

Oxygen isotopes of ^{16}O, ^{17}O, ^{18}O have abundances of 99.758%, 0.038% and 0.204%, respectively (Blunier et al., 2002). $\delta^{17}O$ and $\delta^{18}O$ are used to denote the deviation of measured oxygen isotopes from the standard. Atmospheric O_2 is usually chosen as the standard for TOI method (Barkan and Luz, 2003). The δ is defined as:

$$\delta = (R_{sam} / R_{std} - 1) \times 10^3 \quad , \tag{1}$$

Where R refers to the ratio of heavy isotope (^{17}O or ^{18}O) to the light isotope (^{16}O). Subscripts sam and std refer to sample and standard, respectively. $\delta^{17}O$ and $\delta^{18}O$ are expressed in per mil (‰).

$\Delta^{17}O$ is denoted as the degree of oxygen isotopic anomaly off mass-dependent fractionation. It is a very small value, usually multiplied by 10^6, and represented in per meg (1 per meg = 0.001‰). $\Delta^{17}O$ of standard air O_2 is nil. Although represented in several ways (Kaiser, 2011), $\Delta^{17}O$ can be defined most commonly as equation 2 (Miller, 2002; Luz and Barkan, 2005).

$$\Delta^{17}O = \ln(\delta^{17}O + 1) - \lambda \ln(\delta^{18}O + 1) \, , \tag{2}$$

λ is the mass-dependent fractionation slope, which varies slightly from 0.506 to 0.521 in different biological and isotopic fractionation processes (Luz and Barkan, 2005) (as is shown in Table 1). Most processes in nature discriminates against ^{17}O by about 0.52 times as much as it discriminates against ^{18}O in a mass-dependent way (Thiemens and Meagher, 1984; Miller, 2002). However, photochemical processes (as follows) occurring in the stratosphere among O_2, CO_2 and O_3 result in low $\delta^{17}O$ and $\delta^{18}O$ of O_2 in a mass-independent way (Thiemens and Heidenreich, 1983; Thiemens et al., 1991; Yung et al., 1991), and the λ anomalously turns to 1.7 (Lämmerzahl et al., 2002;

Table 1 λ for different mass-dependent processes associated with biological productivity

Respiration process	λ
Dark respiration	0.516 ± 0.001[a, b]
Alternative way	0.514 ± 0.001[a]
Photorespiration	0.509 ± 0.001[b, c]
Mehler reaction	0.525 ± 0.002[b]
Evapotranspiration (*h*=relative humidity)	(−0.0078±0.0026) * *h*+ 0.5216±0.0008[d]

Notes: [a] Angert et al. (2003); [b] Helman et al. (2005); [c] Sarma et al. (2005); [d] Landais et al. (2006).

Boering et al., 2004).

$$O_2 + UV \rightarrow 2O,$$
$$O + O_2 \rightarrow O_3,$$
$$O_3 + UV \rightarrow O_2 + O(^1D),$$
$$CO_2 + O(^1D) \rightarrow CO_3,$$
$$CO_3 \rightarrow CO_2 + O(^3P),$$
$$O + O \rightarrow O_2.$$

Where the UV is ultraviolet, O (^{1}D) is an excited oxygen atom, and O (^{3}P) is a transient oxygen atom.

High-precision determination of λ can help tracing small $\Delta^{17}O$ variations (Assonov and Brenninkmeijer, 2005). Studies that analyzed isotopic composition of atmospheric oxygen in ice-core bubbles preferred to use λ = 0.516, while in marine dissolved oxygen preferentially used λ = 0.518 (Luz and Barkan, 2005; Barkan and Luz, 2011).

2.2 Assessing past global biospheric production through TOIs in ice-core bubbles

Gas phase photochemical reactions in stratosphere imparts mass-independently fractionated O_2 to the atmosphere, while respiration removes O_2 and photosynthesis replaces the ambient anomalous atmospheric O_2 with mass dependent fractionated O_2. Relative rates of biological O_2 and stratospheric O_2 can determine the relationship between $\delta^{17}O$ and $\delta^{18}O$ of atmospheric O_2 (Luz et al., 1999; Blunier et al., 2002). $\Delta^{17}O$ calculated from paleo atmospheric O_2 accompanied with data on the atmospheric CO_2 concentration can be used to infer variations in past biosphere productivity at the global scale. At a steady state, the oxygen isotopic mass balance is represented as equation 3 (Landais et al. 2007a, 2007b):

$$F_{bio} \times (\Delta^{17}O_{bio} - \Delta^{17}O_{atm}) = F_{strat} \times (\Delta^{17}O_{strat} - \Delta^{17}O_{atm}), \quad (3)$$

Where $\Delta^{17}O_{bio}$ and $\Delta^{17}O_{strat}$ are $\Delta^{17}O$ of biological O_2 flux (F_{bio}) and stratospheric O_2 flux (F_{strat}), respectively. $\Delta^{17}O_{atm}$ is measured from air samples. The ratio of biospheric O_2 production in the past to the present is calculated from equation 4 (Landais et al., 2007a, 2007b):

$$\frac{F_{bio,past}}{F_{bio,prst}} = \frac{F_{strat,past} \times (\Delta^{17}O_{strat,past} - \Delta^{17}O_{atm,past})}{F_{strat,prst} \times (\Delta^{17}O_{strat,prst} - \Delta^{17}O_{atm,prst})} \times \frac{(\Delta^{17}O_{bio,prst} - \Delta^{17}O_{atm,prst})}{(\Delta^{17}O_{bio,past} - \Delta^{17}O_{atm,past})}, \quad (4)$$

Here, subscripts bio, strat, atm, past, prst represent biosphere, stratosphere, atmosphere, the past and the present, respectively. $\Delta^{17}O_{atm,prst}$ is defined as 0, and $\Delta^{17}O_{atm,past}$ is measurable. The former part in the right side of equation 4 can be represented as known CO_2 concentrations ratio of the past to the present (Luz et al., 1999). Equation 4 is now simplified as an equation relevant to $\Delta^{17}O_{bio,prst}$ and $\Delta^{17}O_{bio,past}$, which are determined from both terrestrial ($\Delta^{17}O_{terr}$) and oceanic ($\Delta^{17}O_{ocean}$) biosphere (equation 5; Landais et al., 2007a).

$$\Delta^{17}O_{bio} = \frac{F_{ocean} \times \Delta^{17}O_{ocean} + F_{terr} \times \Delta^{17}O_{terr}}{F_{ocean} + F_{terr}} = \frac{\frac{F_{ocean}}{F_{terr}}\Delta^{17}O_{ocean} + \Delta^{17}O_{terr}}{\frac{F_{ocean}}{F_{terr}} + 1}, \quad (5)$$

Where F_{ocean} and F_{terr} represent the fluxes of oceanic and terrestrial oxygen production, respectively. F_{ocean}/F_{terr} ratio in ocean and terrestrial biosphere varied from 0.45 to 0.59 (Bender et al., 1994; Blunier et al., 2002; Hoffmann et al., 2004). The modern $\Delta^{17}O_{ocean}$ is around 249 meg^{-1} (Luz and Barkan, 2000). More details on calculating $\Delta^{17}O_{terr}$ and $\Delta^{17}O_{ocean}$ in the past and $\Delta^{17}O_{terr}$ at present can be found in Landais et al. (2007a).

2.3 Calculating gross oxygen production through the TOIs of dissolved oxygen in ocean

TOI in the oceanic ML is affected by photosynthesis, respiration, air-sea gas exchange and physical transports among water masses. Respiration effect is eliminated because of bearing the same λ (0.518) as $\Delta^{17}O$ calculation. Physical transports in the ML are assumed to be neglected. Therefore, the magnitude of the $\Delta^{17}O$ in dissolved oxygen is determined by the relative rates of photosynthetic O_2 to air-sea exchange O_2. Dissolved O_2 produced only from photosynthetic splitting of water bears the same isotopic composition as the seawater (Guy et al., 1989; Yakir et al., 1994), and results in a high $\Delta^{17}O$ ($\Delta^{17}O_p$) to 249 ± 15 meg^{-1} (Luz and Barkan, 2000). Dissolved O_2 in equilibrium with atmospheric O_2 bears a low $\Delta^{17}O$ ($\Delta^{17}O_{eq}$) due to air-sea gas exchange. Luz and Barkan (2009) concluded that $\Delta^{17}O_{eq}$ is positively relative to water temperature ($\Delta^{17}O_{eq}$ =0.6×T + 1.8). Measured $\Delta^{17}O$ of dissolved oxygen in ML ($\Delta^{17}O_{diss}$)

falls between the two end-members (van der Meer, 2015; Nicholson et al., 2014). One can thus calculate GOP from $\Delta^{17}O_{diss}$, along with the parameterized k estimated from wind speed (Watson et al., 1991; Behrenfeld and Falkowski, 1997; Nightingale et al., 2000; Sweeney et al., 2007; Ho et al., 2011).

$$GOP = k[O_2]_{eq}\left[\frac{\Delta^{17}O_{diss} - \Delta^{17}O_{eq}}{\Delta^{17}O_p - \Delta^{17}O_{diss}}\right], \quad (6)$$

Here, $[O_2]_{eq}$ is the equilibrium concentration of O_2 (Garcia and Gordon, 1992; Hamme and Emerson, 2004). First proposed by Luz and Barkan (2000), equation (6) is sensitive to errors in $\Delta^{17}O_{diss}$, $\Delta^{17}O_{eq}$, and especially in k. Thus, Prokopenko et al. (2011) proposed the equation (7), which decreases errors for GOP calculation.

$$GOP = k[O_2]_{eq}\frac{\left(1-\frac{10^{-3}\delta^{17}O_{eq}+1}{10^{-3}\delta^{17}O_{diss}+1}\right)-\lambda\left(1-\frac{10^{-3}\delta^{18}O_{eq}+1}{10^{-3}\delta^{18}O_{diss}+1}\right)}{\left(\frac{10^{-3}\delta^{17}O_p+1}{10^{-3}\delta^{17}O_{diss}+1}-1\right)-\lambda\left(\frac{10^{-3}\delta^{18}O_p+1}{10^{-3}\delta^{18}O_{diss}+1}-1\right)}, \quad (7)$$

Where the subscripts p, diss and eq refer to O_2 produced by photosynthesis, dissolved in mixed layer and equilibrated with air, respectively. GOP values calculated by equation (7) are marked with * in Table 3.

3 Methods

Air samples from ice-core bubbles and sea water are collected in pre-evacuated 125 cm^3 and 500 mL glass flasks sealed with the same Louwers Hapert® O-ring stopcocks. Seawater samples are pre-poisoned with 100 μL of $HgCl_2$ saturated solution to avoid biological activity. After 24 hours' equilibration at room temperature, the water is sucked out leaving only headspace gases inside (Emerson et al., 1995; Sarma et al., 2003; Ash et al., 2020). O_2 and Ar are separated from air samples through the separation line in Figure 1.

More details of automatic gas separation can be found in Barkan and Luz (2003). Briefly, H_2O, N_2O and CO_2 are cryogenically removed by T1 and T2 (Dewar flasks with liquid nitrogen) in 5 min, leaving N_2, O_2 and Ar trapped by molecular sieves at −196°C in T3. Carried by pure helium gas, N_2 is separated through the chromatographic column (GC) in T4, leaving O_2 and Ar mixture trapped in T5. By heating the molecular sieves in T5, the gas mixture is then eluted and transferred to the collection finger immersed in T6.

The mixed O_2 and Ar are analyzed in the dual-inlet mass spectrometry by simultaneously measuring m/z 32, 33, and 34 (Abe and Yoshida, 2003). The average standard analytical errors of $\delta^{17}O$, $\delta^{18}O$ and $\Delta^{17}O$ are about 0.006‰, 0.003‰ and 7 meg^{-1} (standard deviation), respectively (Luz et al., 1999; Sarma et al., 2005; Juranek and Quay, 2010; Munro et al., 2013; Keedakkadan and Abe, 2015).

4 Progress on research of triple isotopes of O_2 trapped in ice-core bubbles and dissolved in ocean

4.1 Assessing past global biological productivity through triple isotopes of O_2 trapped in ice-core bubbles

The triple isotopic composition of O_2 from paleo air occluded in ice-core bubbles can be used to estimate the rates of total biological productivity in the past to the present, although uncertainties still remain for terrestrial

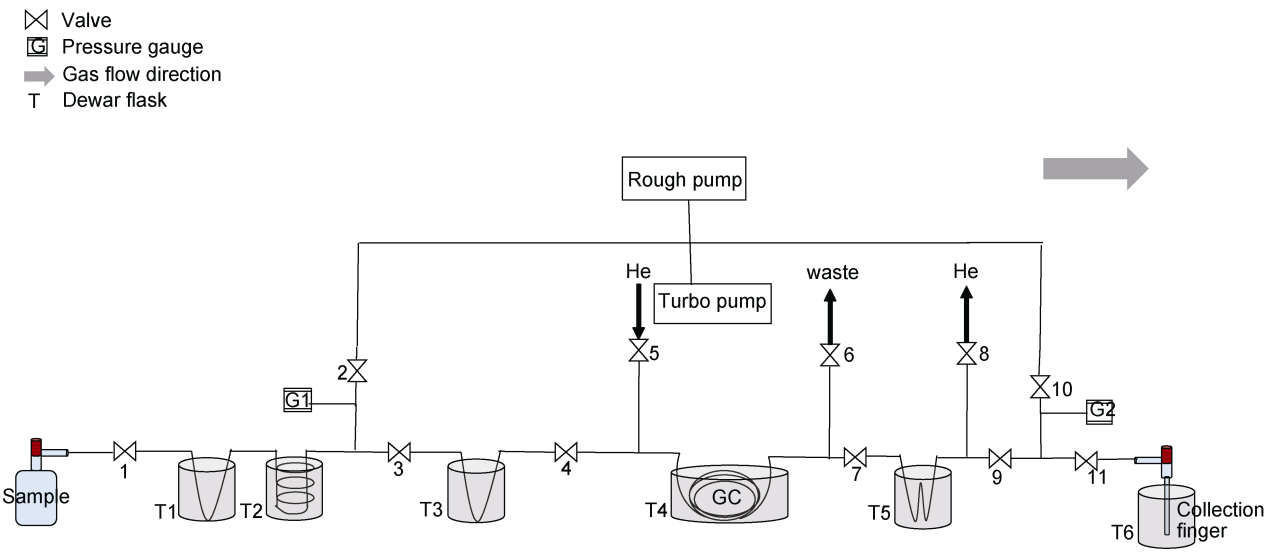

Figure 1 Plot of the separation line.

productivity measurement (Luz et al., 1999; Blunier et al., 2002; Angert et al., 2003; Landais et al., 2007a, 2007b). Here we select records from the Vostok and Greenland Ice Sheet Project 2 (GISP2) as representatives of ice cores in Antarctic and Arctic. The ratios of GOP in the past to the present and $\Delta^{17}O$ values of paleo-atmospheric O_2 are shown in Table 2, and temporal variations of $\Delta^{17}O$ values in past glacial and interglacial times are shown in Figure 2.

Table 2 Ratios of GOP in the past to the present and $\Delta^{17}O$ values of O_2 from ice-core bubbles

Ice core station	Time before the present/ka	Lat, Lon	GOP in the past compared to the present	GOP in the LGM compared to the present	$\Delta^{17}O/(meg^{-1})$	References
GISP2	82.03	72.58°N, 38.48°E	0.87−0.97		12	Luz et al., 1999
	56.17				35	
	36.67				21	
	25.78			0.9	39	
	18.67			0.9	37	
	0.15				0	
GISP2	60−42	72.58°N, 38.48°E	/		30	Blunier et al., 2002
	24−16			0.76−0.83	38	
	16−12.5			0.76−0.83	22	
	12.5−5				3	
	5−0				−1	
	0				0	
Vostok	400	78.45°S, 106.83°E	0.94−0.83		40	Blunier et al., 2012
*	LGM	/	/	0.60−0.75	/	Landais et al., 2007a, 2007b
*	LGM	/	/	0.69	43	

Note: * Data referenced from Luz et al. (1999) and Blunier et al. (2002).

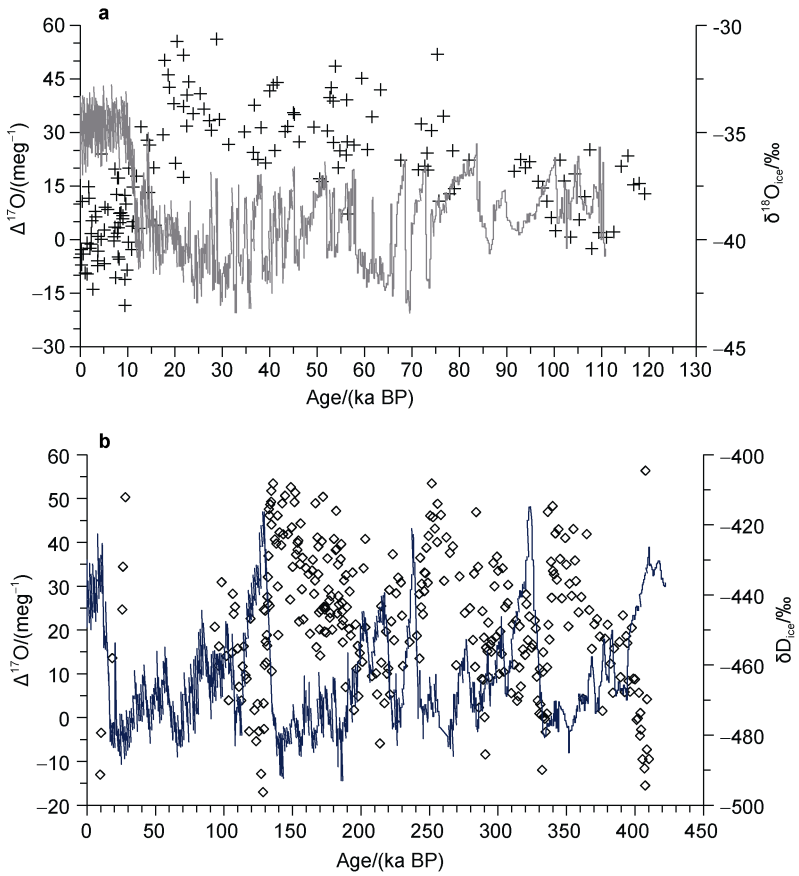

Figure 2 Variations of $\Delta^{17}O$ in O_2 trapped in ice-core bubbles from GISP2 (crosses) (**a**) and Vostok (diamonds) (**b**) at glacial-interglacial timescale (Luz et al., 1999; Blunier et al., 2012). In addition, the ice $\delta^{18}O$ of GISP2 (grey curve; Grootes et al., 1993) and ice δD of Vostok (dark blue curve; Petit et al., 1999) are also shown to indicate the glacial-interglacial cycles.

Luz et al. (1999) first applied the TOI method to estimate the past global biological production through ice cores from GISP2. They concluded that the average estimate of the global GOP ratio in the past 82 ka is 87%–97% of the modern productivity, and proposed that the marine biosphere was almost the same as or just a little higher than the present, while the terrestrial biosphere was slightly lower. Blunier et al. (2002) also calculated the $\Delta^{17}O$ of paleo-atmospheric O_2 trapped in ice-core bubbles from GISP2 over the last 60 ka, and concluded that the GOP rates are only~76%–83% of the modern for the LGM and are slightly lower than today for the glacial-interglacial transition and the early Holocene. Landais et al. (2007a) calculated the biological productivity ratio for the LGM as 60%–75%, and proposed that estimates of the LGM oxygen biosphere productivity obtained by Blunier et al. (2002) may not be adequate (Hoffmann et al., 2004) compared with that in Luz et al. (1999), because of various climatic conditions and plant coverage (Hoffmann et al., 2004). Landais et al. (2007b) emphasized on the relationship between $\delta^{17}O$ and $\delta^{18}O$ during leaf transpiration, and concluded that the GOP rate during the LGM is 69%±6% of the present, and yielded that the $\Delta^{17}O$ is constant around 40 meg^{-1} in glacial times, while changed a lot in the LGM.

Blunier et al. (2012) calculated biospheric productivity from 400 ka BP $\Delta^{17}O$ records in Vostok, and concluded that the mean GOP ratios during the past 400 ka are 94%–83% of the modern rates. They also found that oceanic oxygen productivity was elevated by ~20% relative to the present during glacial maximum and the transition of glacial-interglacial, but the increase did not compensate for land productivity decrease.

The variations of biogenic productivity over paleo times in the ocean biosphere are different from that in the land biosphere, especially in glacial times. Blunier et al. (2012) concluded that there were still uncertainties remained to assess both land and ocean productivities from $\Delta^{17}O$ data of O_2. Distinguished from the global mean value, the marine biological production in glacial times were 88%–140% of the present (Luz et al., 1999; Blunier et al., 2002), while terrestrial biosphere remained uncertain because of complex plant physiology. Angert et al. (2003) showed that at least 15% of the changes in the triple oxygen isotopic composition in paleo-air should be related to the variations among different respiration mechanisms.

4.2 Assessing marine photosynthetically produced oxygen through triple isotopes of O_2 dissolved in ocean

The TOI method has been widely applied to measure marine primary productivity in the ML of global open ocean or coastal ocean. Specifically, spatial distribution of TOI-GOP study sites in global ocean is illustrated in Figure 3, and the mean TOI-GOP values are presented in Table 3. According to Juranek and Quay (2010), gross primary productivity (GPP) data were all converted to GOP data based on the photosynthetic quotient (PQ = 1.2) (Burris, 1981; Laws, 1991) and a 15% correction (Bender et al., 1999; Laws et al., 2000) (GPP = GOP × (0.85/PQ)). TOI-GOP data were acquired in the Southern Ocean, the Pacific, the Atlantic and the Arctic oceans, of which the Pacific Ocean and coastal ocean gained wide attention, while the Indian Ocean was blank in TOI-GOP values. So far, TOI-based GOP assessment in the subtropical Atlantic and the subtropical Pacific has mainly collected data from the Bermuda Atlantic Time-series Station (BATS) and the Hawaii Ocean Time-series Station ALOHA, respectively.

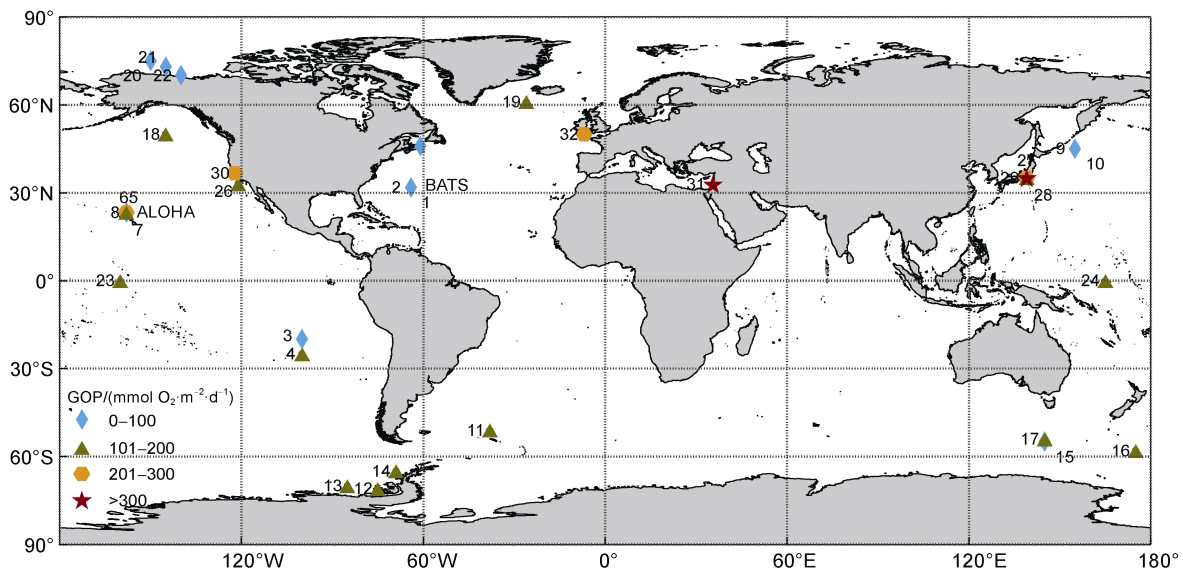

Figure 3 Distribution of TOI-derived GOP values in different oceanic zones.

Table 3 TOI-GOP calculations in different ocean zones

Global ocean zones	No.	Study region/Time interval	Selected point (this study)	Averaged GOP/(mmol $O_2 \cdot m^{-2} \cdot d^{-1}$)	Bias/(mmol $O_2 \cdot m^{-2} \cdot d^{-1}$)	References
Subtropical Atlantic	1	BATS (31.83°N, 64.10°W), Jul 1998–Jul 1999	31.83°N, 64.10°W	82.5^{+}	23	Luz and Barkan, 2000
	2	BATS (31.83°N, 64.10°W), Mar 2000–Jan 2001	31.83°N, 64.10°W	61.85	0	Luz and Barkan, 2009
Subtropical Pacific	3	Southern Pacific Gyre Apr 2011	20°S, 100°W	74^{+}	27	Haskell et al., 2016
	4	Southern subtropics (10°S–20°/30°S), Aug 2004–Nov 2005	25°S, 100°W	115	7	Juranek and Quay, 2010
	5	Northern Subtropics (10°N–30°N, 160°E–120°W), Aug 2004–Nov 2005	23.25°N, 158°W	98	8	
	6	HOT-ALOHA (23.25°N, 158°W), April 2003, Oct 2003, Mar 2006, Aug–Sep 2008	23.25°N, 158°W	99	9	Juranek et al., 2012*
	7	HOT-ALOHA (23.25°N, 158°W), Feb 2002–Aug 2003	23.25°N, 158°W	238.72	0	Juranek and Quay, 2005
	8	HOT-ALOHA (23.25°N, 158°W), Jan 2006–Jan 2008	23.25°N, 158°W	103^{+}	43	Quay et al., 2010
North Pacific	9	The Kyodo North Pacific Time Series (KNOT), Oct 2008–Dec 2012	45°N, 155°E	60	22	Palevsky et al., 2016
	10	Ocean Station Papa (OSP), Oct 2008–Dec 2012	45°N, 155°E	38	10	
Southern Ocean	11	Southwest sector of the SO, Mar 2008	51°S, 38°W	120.5	38	Hamme et al., 2012
	12	West Sea Ice Zone of the Bellingshausen Sea, summer 2007	71°S, 75°W	176	70	Castro-Morales et al., 2013*
	13	Permanent Open Ocean Zone of Bellingshausen Sea, summer 2007	70°S, 85°W	132	49	
	14	West Antarctic Peninsula, Jan 2008	65°S, 69°W	130	90	Huang et al., 2012
	15	Australian sector of the SO (40°S–70°S, 130°E–160°W), Oct–Mar 2007–2010	55°S, 145°E	86	90	Bender et al., 2016*
	16	175°E in Sub-Antarctic Zone in December (47°S–68°S), Oct–Mar 2007–2010	58°S, 175°E	134.5	61	Hendricks et al., 2004
	17	145°E in Sub-Antarctic Zone in December (47°S–68°S), Oct–Mar 2007–2010	54°S, 145°E	190.7	120	
Subpolar North Atlantic	18	Northeast Subarctic region (50°N, 145°W), Apr 2003, Oct 2003, Mar 2006, Aug–Sep 2008	50°N, 145°W	196	16	Juranek et al., 2012
	19	Subpolar North Atlantic (45°N–55°N; 10°W–60°W), May 2008	61°N, 26°W	166.5	45	Quay et al., 2012
Arctic Ocean	20	Beaufort Gyre region of the Canada Basin (70°N–80°N, 130°W–155°W), Late Jul–Aug 2011	75°N, 150°W	38	3	Stanley et al., 2015*
	21	Beaufort Gyre region of the Canada Basin (70°N–80°N, 130°W–155°W), Late Jul–Aug 2012	73°N, 145°W	16	5	

Continued

Global ocean zones	No.	Study region/Time interval	Selected point (this study)	Averaged GOP/(mmol $O_2 \cdot m^{-2} \cdot d^{-1}$)	Bias/(mmol $O_2 \cdot m^{-2} \cdot d^{-1}$)	References
Arctic Ocean	22	Beaufort Gyre region of the Canadian Basin (70°N–81°N, 131°W–176°W), Summer in 2011, 2012, 2013; Fall in 2014, 2015, 2016	70°N, 140°W	54	9	Ji et al., 2019
Equatorial Pacific	23	Equatorial Pacific (10°S–10°N), Aug 2004–Nov 2005	0°, 160°W	200	11	Juranek and Quay, 2010
	24	(140°W–140°E, 2°S–2°N), Aug and Sep 2006	0°, 165°E	121	34	Stanley et al., 2010
Coastal ocean	25	Whycocomagh Bay, Bras d'Or Lake system, 22–31 Mar, 7–28 Apr 2013	46°N, 61°W	5.4	2.2	Manning et al., 2019
	26	Southern California (125°W–117°W, 28°N–34°N), Nov 2005–Aug 2008	33°N, 121°W	151	59	Munro et al., 2013
	27	The Sagami Bay, May, Jun, Aug, Oct 2002	35°N, 139°E	212.1	54	Sarma et al., 2005
	28	The Sagami Bay, 29 Aug 2003, 18–19 Jun 2004, 1–2 Aug 2004	35°N, 139°E	127.74	38	Sarma et al., 2006
	29	The Sagami Bay, 02 May–09 May, 2006	35°N, 139°E	319.9	26	Sarma et al., 2008
	30	Montery Bay, 27 Sep–3 Oct 2014	36.75°N, 122.03°W	209	17	Manning et al., 2017b*
	31	Sea of Galilee, Feb 1998–Feb 1999	32.83°N, 35.58°E	1012.5^{+}	204	Luz and Barkan, 2000
	32	Celtic Sea, Apr 2015	50°N, 7°W	225	115	Seguro et al., 2019

Notes: * GOP calculated from equation (7); $^{+}$ GOP allowing for production below the ML.

In the Southern Ocean, TOI-based GOP values focused on the Antarctic Peninsula and the sector close to Australia.

Although widely applied in global ocean regions, TOI method's assumptions of a steady state (no change of $\Delta^{17}O$ with time) in the ML and no physical transports resulted in potential biases in different regions and seasons. It is apparent from Table 3 that the Southern Ocean bears the largest biases for mean GOP values, followed by the coastal ocean. Luz and Barkan (2009) demonstrated that ocean dynamics will affect the $\Delta^{17}O_{diss}$ in the ML of subtropical ocean on a seasonal scale. Vertical entrainment or mixing of seawater was the largest sources of the bias, and seasonal variability of $\Delta^{17}O_{diss}$ was another significant source. Nicholson et al. (2014) further demonstrated that biases resulted from physical dynamics tended to incur larger overestimation in midlatitudes and in summer and fall, and biases due to seasonal variability were highest in the fall.

Considering the main contribution of physical transports and seasonal variability to GOP biases in the ML, non-steady state GOP terms were proposed to better estimate primary productivity in the euphotic layer or even the deep ocean (Nicholson et al., 2012; Wurgaft et al., 2013). Luz and Barkan (2000) first calculated the TOI-GOP values covering the euphotic zone with the steady state assumption. Kaiser (2011) and Prokopenko et al. (2011) accounted for disequilibrium terms that affected GOP in the ML, and concluded that exact expressions including both non-steady and steady states performed well in high-productivity aquatic ecosystems. Haskell et al. (2016) then applied the exact expression proposed by Prokopenko et al. (2011) in oligotrophic ocean, and found that the disequilibrium terms would slightly affect GOP values in the ML.

Given to the wide range of time and spatial scales that various productivity methods covered, comparisons were needed to explore their applicability in oceans of different space and timescales (Hamme et al., 2012). TOI-based GOP values more or less exceeded values estimated from traditional methods, which uncovered the underestimation of incubation methods on primary productivity. Quay et al. (2010) concluded that the $\Delta^{17}O$-derived GOP exceeded the labeled ^{18}O-GOP by 25%–60%. Reuer et al. (2007) found the TOI-based GOP higher than the prediction in Behrenfeld and Falkowski (1997), and about 2.7 times higher than ^{14}C-based gross production. Globally, the underestimation of primary productivity using incubation methods became the greatest in the tropics (Juranek and

Quay, 2010). Sarma et al. (2005) attributed the underestimation to unavailability of O_2 uptake rates and the assumption of equal light and dark respiration mechanisms.

Apart from the application of TOI for GOP calculation, O_2/Ar ratios can be concomitantly measured to calculate net oxygen productivity (NOP) (Reuer et al., 2007; Castro-Morales et al., 2013; Munro et al., 2013). More studies have also used recently the NOP/GOP ratios to suggest the potential export efficiency of community ecosystems (Juranek and Quay, 2005; Reuer et al., 2007; Luz and Barkan, 2009), especially in high productivity ecosystems (Prokopenko et al., 2011). Detailed calculations for the weighted gas transfer velocity is key to high-precision NOP calculation (Reuer et al., 2007), while NOP/GOP ratios calculation were free from *k* errors, and they were in the range of ^{15}N incubation ratios (Sambrotto and Mace, 2000).

5 Problems and prospects

TOI method has been applied widely in assessing past global primary production and modern marine productivity, but problems still remain on possible biases and inadequate understandings, which awaits improvements in future studies.

(1) The assumption of a steady state and neglected physical transports may cause large biases in productivity calculation, thus future studies await further exploration of complex advective mixing or vertical entrainment of seawater, and combined the steady and non-steady state equation to calculate biospheric production in euphotic layer or even deep ocean.

(2) Calculating $\Delta^{17}O$-based GOP requires accurate gas separation processes and high-precision measurements of $\delta^{18}O$ and $\delta^{17}O$. However, there are only a few technologies in the world that can control the uncertainties and precision in analytically available range. Another big error comes from parameterization of air-sea oxygen exchange rate (Reuer et al., 2007). Thus, more studies need improvements on accurate gas separation and high-precision mass spectrometry analyzing technologies in future works, and a uniform and widely accepted *k* parameterization standard awaits further exploration.

(3) Inadequate understandings still remain in conversion between GOP and GPP. Therefore, relationships between GOP and GPP need to be better understood by tracking O_2 and carbon flows in natural communities over long ranges of timescales (Juranek and Quay, 2013).

(4) Complex physiological mechanisms of terrestrial plants hindered the wide application of TOI method in estimating past global biological production, like the inadequate knowledge of leaf water transpiration (Landais et al. 2007b). Studies in the future can move forward on assessment of past global productivity through $\Delta^{17}O$ signals in ice-core bubbles earlier than 400 ka BP.

Acknowledgements We appreciate the Institute of Oceanography, Shanghai Jiao Tong University, which provides experiment platforms for us to learn about disciplines of gas separation line and high-precision measurements of TOIs. We are grateful to Zhaojun Zhan, Yanyan Cai and Jiajia Wang, for their help on plots. Gratitude also goes to the technicians who gave suggestions on our pre-processed system. This work was supported by the National Natural Science Foundation of China (Grant nos. 41771031 and 41673125) and the Priority Academic Program Development of Jiangsu Higher Education Institutions (PAPD). We would like to thank two anonymous reviewers, and Associate Editor Dr. Cinzia Verde, for their valuable suggestions and comments that improved this article.

References

Abe O, Yoshida N. 2003. Partial pressure dependency of $^{17}O/^{16}O$ and $^{18}O/^{16}O$ of molecular oxygen in the mass spectrometer. Rapid Commun Mass Spectrom, 17(5): 395-400, doi:10.1002/rcm.923.

Angert A, Rachmilevitch S, Barkan E, et al. 2003. Effects of photorespiration, the cytochrome pathway, and the alternative pathway on the triple isotopic composition of atmospheric O_2. Glob Biogeochem Cycles, 17(1): 1030, doi:10.1029/2002GB001933.

Ash J L, Hu H T, Yeung L Y. 2020. What fractionates oxygen isotopes during respiration? Insights from multiple isotopologue measurements and theory. ACS Earth Space Chem, 4(1): 50-66, doi:10.1021/acsearthspacechem.9b00230.

Assonov S S, Brenninkmeijer C A M. 2005. Reporting small $\Delta^{17}O$ values: existing definitions and concepts. Rapid Commun Mass Spectrom, 19(5): 627-636, doi:10.1002/rcm.1833.

Barkan E, Luz B. 2003. High-precision measurements of $^{17}O/^{16}O$ and $^{18}O/^{16}O$ of O_2 and O_2/Ar ratio in air. Rapid Commun Mass Spectrom, 17(24): 2809-2814, doi:10.1002/rcm.1267.

Barkan E, Luz B. 2011. The relationships among the three stable isotopes of oxygen in air, seawater and marine photosynthesis. Rapid Commun Mass Spectrom, 25(16): 2367-2369, doi:10.1002/rcm.5125.

Behrenfeld M J, Falkowski P G. 1997. Photosynthetic rates derived from satellite-based chlorophyll concentration. Limnol Oceanogr, 42(1): 1-20, doi:10.4319/lo.1997.42.1.0001.

Bender M, Grande K, Johnson K, et al. 1987. A comparison of four methods for determining planktonic community production. Limnol Oceanogr, 32(5): 1085-1098, doi:10.4319/lo.1987.32.5.1085.

Bender M, Orchardo J, Dickson M L, et al. 1999. *In vitro* O_2 fluxes compared with ^{14}C production and other rate terms during the JGOFS Equatorial Pacific experiment. Deep Sea Res Part I: Oceanogr Res Pap, 46(4): 637-654, doi:10.1016/s0967-0637(98)00080-6.

Bender M, Sowers T, Labeyrie L. 1994. The Dole Effect and its variations during the last 130, 000 years as measured in the Vostok Ice Core. Glob Biogeochem Cycles, 8(3): 363-376, doi:10.1029/94GB00724.

Bender M L, Tilbrook B, Cassar N, et al. 2016. Ocean productivity south of Australia during spring and summer. Deep Sea Res Part I: Oceanogr Res Pap, 112: 68-78, doi:10.1016/j.dsr.2016.02.018.

Blunier T, Barnett B, Bender M L, et al. 2002. Biological oxygen productivity during the last 60, 000 years from triple oxygen isotope measurements. Glob Biogeochem Cycles, 16(3): 3-1-3-13, doi:10.1029/ 2001GB001460.

Blunier T, Bender M L, Barnett B, et al. 2012. Planetary fertility during the

past 400 ka based on the triple isotope composition of O_2 in trapped gases from the Vostok ice core. Clim Past, 8(5): 1509-1526, doi:10.5194/cp-8-1509-2012.

Boering K A, Jackson T, Hoag K J, et al. 2004. Observations of the anomalous oxygen isotopic composition of carbon dioxide in the lower stratosphere and the flux of the anomaly to the troposphere. Geophys Res Lett, 31(3): L03109, doi:10.1029/2003GL018451.

Burris J E. 1981. Effects of oxygen and inorganic carbon concentrations on the photosynthetic quotients of marine algae. Mar Biol, 65(3): 215-219, doi:10.1007/BF00397114.

Castro-Morales K, Cassar N, Shoosmith D R, et al. 2013. Biological production in the Bellingshausen Sea from oxygen-to-argon ratios and oxygen triple isotopes. Biogeosciences, 10(4): 2273-2291, doi:10.5194/bg-10-2273-2013.

Emerson S, Quay P D, Stump C, et al. 1995. Chemical tracers of productivity and respiration in the subtropical Pacific Ocean. J Geophys Res: Oceans, 100(C8): 15873-15887, doi:10.1029/95JC 01333.

Fujiki T, Hosaka T, Kimoto H, et al. 2008. *In situ* observation of phytoplankton productivity by an underwater profiling buoy system: use of fast repetition rate fluorometry. Mar Ecol Prog Ser, 353: 81-88, doi:10.3354/meps07151.

Garcia H E, Gordon L I. 1992. Oxygen solubility in seawater: better fitting equations. Limnol Oceanogr, 37(6): 1307-1312, doi:10.4319/lo.1992.37.6.1307.

Grande K D, Williams P J L, Marra J, et al. 1989. Primary production in the North Pacific Gyre: a comparison of rates determined by the ^{14}C, O_2 concentration and ^{18}O methods. Deep Sea Res A Oceanogr Res Pap, 36(11): 1621-1634, doi:10.1016/0198-0149(89)90063-0.

Grootes P M, Stuiver M, White J W C, et al. 1993. Comparison of oxygen isotope records from the GISP2 and GRIP Greenland ice cores. Nature, 366(6455): 552-554, doi:10.1038/366552a0.

Guy R D, Berry J A, Fogel M L, et al. 1989. Differential fractionation of oxygen isotopes by cyanide-resistant and cyanide-sensitive respiration in plants. Planta, 177(4): 483-491, doi:10.1007/BF00392616.

Hamme R C, Cassar N, Lance V P, et al. 2012. Dissolved O_2/Ar and other methods reveal rapid changes in productivity during a Lagrangian experiment in the Southern Ocean. J Geophys Res: Oceans, 117(C4): C00F12, doi:10.1029/2011JC007046.

Hamme R C, Emerson S R. 2004. The solubility of neon, nitrogen and argon in distilled water and seawater. Deep Sea Res Part I: Oceanogr Res Pap, 51(11): 1517-1528, doi:10.1016/j.dsr.2004.06.009.

Harris G P, Griffiths F B, Thomas D P. 1989. Light and dark uptake and loss of ^{14}C: methodological problems with productivity measurements in oceanic waters. Hydrobiologia, 173(2): 95-105, doi:10.1007/BF000 15519.

Harrison W G, Harris L R. 1986. Isotope-dilution and its effects on measurements of nitrogen and phosphorus uptake by oceanic microplankton. Mar Ecol Prog Ser, 27: 253-261, doi:10.3354/meps027253.

Haskell II W Z, Prokopenko M G, Stanley R H R, et al. 2016. Estimates of vertical turbulent mixing used to determine a vertical gradient in net and gross oxygen production in the oligotrophic South Pacific Gyre. Geophys Res Lett, 43(14): 7590-7599, doi:10.1002/2016GL069523.

Helman Y, Barkan E, Eisenstadt D, et al. 2005. Fractionation of the three stable oxygen isotopes by oxygen-producing and oxygen-consuming reactions in photosynthetic organisms. Plant Physiol, 138(4): 2292-2298, doi:10.1104/pp.105.063768.

Hendricks M B, Bender M L, Barnett B A. 2004. Net and gross O_2 production in the southern ocean from measurements of biological O_2 saturation and its triple isotope composition. Deep Sea Res Part I: Oceanogr Res Pap, 51(11): 1541-1561, doi:10.1016/j.dsr.2004.06.006.

Hendricks M B, Bender M L, Barnett B A, et al. 2005. Triple oxygen isotope composition of dissolved O_2 in the equatorial Pacific: a tracer of mixing, production, and respiration. J Geophys Res: Oceans, 110(C12): C12021, doi:10.1029/2004JC002735.

Ho D T, Wanninkhof R, Schlosser P, et al. 2011. Toward a universal relationship between wind speed and gas exchange: Gas transfer velocities measured with $^3He/SF_6$ during the Southern Ocean Gas Exchange Experiment. J Geophys Res: Oceans, 116(C4): C00F04, doi:10.1029/2010JC006854.

Hoffmann G, Cuntz M, Weber C, et al. 2004. A model of the Earth's Dole effect. Global Biogeochem Cycles, 18(1): GB1008, doi:10.1029/2003gb002059.

Hotchkiss E R, Hall R O. 2014. High rates of daytime respiration in three streams: Use of $\delta^{18}O_{O_2}$ and O_2 to model diel ecosystem metabolism. Limnol Oceanogr, 59(3): 798-810, doi:10.4319/lo.2014.59.3.0798.

Howard E M, Spivak A C, Karolewski J S, et al. 2020. Oxygen and triple oxygen isotope measurements provide different insights into gross oxygen production in a shallow salt marsh pond. Estuaries Coasts, 43(8): 1908-1922, doi:10.1007/s12237-020-00757-6.

Huang K, Ducklow H, Vernet M, et al. 2012. Export production and its regulating factors in the West Antarctica Peninsula region of the Southern Ocean. Glob Biogeochem Cycles, 26(2): GB2005, doi:10.1029/2010GB004028.

IPCC. 2014. Climate Change 2014: Synthesis report. IPCC, Geneva, Switzerland.

Ji B Y, Sandwith Z O, Williams W J, et al. 2019. Variations in rates of biological production in the Beaufort Gyre as the Arctic changes: rates from 2011 to 2016. J Geophys Res: Oceans, 124(6): 3628-3644, doi:10.1029/2018JC014805.

Juranek L W, Quay P D. 2005. *In vitro* and *in situ* gross primary and net community production in the North Pacific Subtropical Gyre using labeled and natural abundance isotopes of dissolved O_2. Glob Biogeochem Cycles, 19(3): GB3009, doi:10.1029/2004GB002384.

Juranek L W, Quay P D. 2010. Basin-wide photosynthetic production rates in the subtropical and tropical Pacific Ocean determined from dissolved oxygen isotope ratio measurements. Glob Biogeochem Cycles, 24(2): GB2006, doi:10.1029/2009GB003492.

Juranek L W, Quay P D. 2013. Using triple isotopes of dissolved oxygen to evaluate global marine productivity. Ann Rev Mar Sci, 5: 503-524, doi:10.1146/annurev-marine-121211-172430.

Juranek L W, Quay P D, Feely R A, et al. 2012. Biological production in the NE Pacific and its influence on air-sea CO_2 flux: Evidence from dissolved oxygen isotopes and O_2/Ar. J Geophys Res: Oceans, 117(C5): C05022, doi:10.1029/2011JC007450.

Jurikova H, Guha T, Abe O, et al. 2016. Variations in triple isotope composition of dissolved oxygen and primary production in a subtropical reservoir. Biogeosciences, 13(24): 6683-6698, doi:10.5194/bg-13-6683-2016.

Kaiser J. 2011. Technical note: Consistent calculation of aquatic gross production from oxygen triple isotope measurements. Biogeosciences, 8(7): 1793-1811, doi:10.5194/bg-8-1793-2011.

Keedakkadan H R, Abe O. 2015. Cryogenic separation of an oxygen-argon

mixture in natural air samples for the determination of isotope and molecular ratios. Rapid Commun Mass Spectrom, 29(8): 775-781, doi:10.1002/rcm.7161.

Lämmerzahl P, Röckmann T, Brenninkmeijer C A M, et al. 2002. Oxygen isotope composition of stratospheric carbon dioxide. Geophys Res Lett, 29(12): 1582, doi:10.1029/2001GL014343.

Landais A, Barkan E, Yakir D, et al. 2006. The triple isotopic composition of oxygen in leaf water. Geochimica et Cosmochimica Acta, 70(16): 4105-4115, doi:10.1016/j.gca.2006.06.1545.

Landais A, Lathiere J, Barkan E, et al. 2007a. Reconsidering the change in global biosphere productivity between the Last Glacial Maximum and present day from the triple oxygen isotopic composition of air trapped in ice cores. Glob Biogeochem Cycles, 21(1): GB1025, doi:10.1029/2006GB002739.

Landais A, Yakir D, Barkan E, et al. 2007b. The triple isotopic composition of oxygen in leaf water and its implications for quantifying biosphere productivity. Terr Ecol, 1: 111-125, doi:10.1016/s1936-7961(07)01008-1.

Laws E A. 1991. Photosynthetic quotients, new production and net community production in the open ocean. Deep Sea Res A: Oceanogr Res Pap, 38(1): 143-167, doi:10.1016/0198-0149(91)90059-O.

Laws E A, Landry M R, Barber R T, et al. 2000. Carbon cycling in primary production bottle incubations: inferences from grazing experiments and photosynthetic studies using ^{14}C and ^{18}O in the Arabian Sea. Deep Sea Res Part II: Top Stud Oceanogr, 47(7-8): 1339-1352, doi:10.1016/S0967-0645(99)00146-0.

Li B D, Yeung L Y, Hu H T, et al. 2019. Kinetic and equilibrium fractionation of O_2 isotopologues during air-water gas transfer and implications for tracing oxygen cycling in the ocean. Mar Chem, 210: 61-71, doi:10.1016/j.marchem.2019.02.006.

Luz B, Barkan E. 2000. Assessment of oceanic productivity with the triple-isotope composition of dissolved oxygen. Science, 288(5473): 2028-2031, doi:10.1126/science.288.5473.2028.

Luz B, Barkan E. 2005. The isotopic ratios $^{17}O/^{16}O$ and $^{18}O/^{16}O$ in molecular oxygen and their significance in biogeochemistry. Geochimica et Cosmochimica Acta, 69(5): 1099-1110, doi:10.1016/j.gca.2004.09.001.

Luz B, Barkan E. 2009. Net and gross oxygen production from O_2/Ar, $^{17}O/^{16}O$ and $^{18}O/^{16}O$ ratios. Aquat Microb Ecol, 56: 133-145, doi:10.3354/ame01296.

Luz B, Barkan E, Bender M L, et al. 1999. Triple-isotope composition of atmospheric oxygen as a tracer of biosphere productivity. Nature, 400(6744): 547-550, doi:10.1038/22987.

Luz B, Barkan E, Sagi Y, et al. 2002. Evaluation of community respiratory mechanisms with oxygen isotopes: a case study in Lake Kinneret. Limnol Oceanogr, 47(1): 33-42, doi:10.4319/lo.2002.47.1.0033.

Manning C C, Howard E M, Nicholson D P, et al. 2017a. Revising estimates of aquatic gross oxygen production by the triple oxygen isotope method to incorporate the local isotopic composition of water. Geophys Res Lett, 44(20): 10511-10519, doi:10.1002/2017GL074375.

Manning C C, Stanley R H R, Nicholson D P, et al. 2017b. Impact of recently upwelled water on productivity investigated using *in situ* and incubation-based methods in Monterey Bay. J Geophys Res: Oceans, 122(3): 1901-1926, doi:10.1002/2016JC012306.

Manning C C, Stanley R H R, Nicholson D P, et al. 2019. Changes in gross oxygen production, net oxygen production, and air-water gas exchange during seasonal ice melt in Whycocomagh Bay, a Canadian estuary in the Bras d'Or Lake system. Biogeosciences, 16(17): 3351-3376, doi:10.5194/bg-16-3351-2019.

Marra J. 2007. Approaches to the measurement of plankton production// Williams P J l B, Thomas D N, Reynolds C S. Phytoplankton productivity. Oxford, UK: Blackwell Science Ltd, 78-108, doi:10.1002/9780470995204.ch4.

Miller M F. 2002. Isotopic fractionation and the quantification of ^{17}O anomalies in the oxygen three-isotope system: an appraisal and geochemical significance. Geochimica et Cosmochimica Acta, 66(11): 1881-1889, doi:10.1016/S0016-7037(02)00832-3.

Reuer M K, Barnett B A, Bender M L, et al. 2007. New estimates of Southern Ocean biological production rates from O_2/Ar ratios and the triple isotope composition of O_2. Deep Sea Res Part I: Oceanogr Res Pap, 54(6): 951-974, doi:10.1016/j.dsr.2007.02.007.

Munro D R, Quay P D, Juranek L W, et al. 2013. Biological production rates off the Southern California Coast estimated from triple O_2 isotopes and O_2: Ar gas ratios. Limnol Oceanogr, 58(4): 1312-1328, doi:10.4319/lo.2013.58.4.1312.

Moore C M, Suggett D, Holligan P M, et al. 2003. Physical controls on phytoplankton physiology and production at a shelf sea front: a fast repetition-rate fluorometer based field study. Mar Ecol Prog Ser, 259: 29-45, doi:10.3354/meps259029.

Nicholson D P, Stanley R H R, Barkan E, et al. 2012. Evaluating triple oxygen isotope estimates of gross primary production at the Hawaii Ocean Time-series and Bermuda Atlantic Time-series Study sites. J Geophys Res: Oceans, 117(C5): C05012, doi:10.1029/2010JC006856.

Nicholson D, Stanley R H R, Doney S C. 2014. The triple oxygen isotope tracer of primary productivity in a dynamic ocean model. Glob Biogeochem Cycles, 28(5): 538-552, doi:10.1002/2013GB004704.

Nielsen E S. 1952. The use of radio-active carbon (^{14}C) for measuring organic production in the sea. ICES Journal of Marine Science, 18(2): 117-140, doi:10.1093/icesjms/18.2.117.

Nightingale P D, Malin G, Law C S, et al. 2000. *In situ* evaluation of air-sea gas exchange parameterizations using novel conservative and volatile tracers. Glob Biogeochem Cycles, 14(1): 373-387, doi:10.1029/1999GB900091.

Palevsky H I, Quay P D, Lockwood D E, et al. 2016. The annual cycle of gross primary production, net community production, and export efficiency across the North Pacific Ocean. Glob Biogeochem Cycles, 30(2): 361-380, doi:10.1002/2015GB005318.

Peterson B J. 1980. Aquatic primary productivity and the ^{14}C-CO_2 method: a history of the productivity problem. Annu Rev Ecol Syst, 11(1): 359-385, doi:10.1146/annurev.es.11.110180.002043.

Petit J R, Jouzel J, Raynaud D, et al. 1999. Climate and atmospheric history of the past 420, 000 years from the Vostok ice core, Antarctica. Nature, 399(6735): 429-436, doi:10.1038/20859.

Prokopenko M G, Pauluis O M, Granger J, et al. 2011. Exact evaluation of gross photosynthetic production from the oxygen triple-isotope composition of O_2: Implications for the net-to-gross primary production ratios. Geophys Res Lett, 38(14): L14603, doi:10.1029/2011GL047652.

Quay P D, Emerson S, Wilbur D O, et al. 1993. The $\delta^{18}O$ of dissolved O_2 in the surface waters of the subarctic Pacific: a tracer of biological productivity. J Geophys Res, 98(C5): 8447-8458, doi:10.1029/92jc 03017.

Quay P D, Peacock C, Björkman K, et al. 2010. Measuring primary production rates in the ocean: Enigmatic results between incubation

and non-incubation methods at Station ALOHA. Glob Biogeochem Cycles, 24(3): GB3014, doi:10.1029/2009GB003665.

Quay P, Stutsman J, Steinhoff T. 2012. Primary production and carbon export rates across the subpolar N. Atlantic Ocean basin based on triple oxygen isotope and dissolved O_2 and Ar gas measurements. Glob Biogeochem Cycles, 26(2): GB2003, doi:10.1029/2010GB 004003.

Sambrotto R N, Mace B J. 2000. Coupling of biological and physical regimes across the Antarctic Polar Front as reflected by nitrogen production and recycling. Deep Sea Res Part II: Top Stud Oceanogr, 47(15-16): 3339-3367, doi:10.1016/S0967-0645(00)00071-0.

Sarma V V S S, Abe O, Hashimoto S, et al. 2005. Seasonal variations in triple oxygen isotopes and gross oxygen production in the Sagami Bay, central Japan. Limnol Oceanogr, 50(2): 544-552, doi:10.4319/lo.2005. 50.2.0544.

Sarma V V S S, Abe O, Hinuma A, et al. 2006. Short-term variation of triple oxygen isotopes and gross oxygen production in the Sagami Bay, central Japan. Limnol Oceanogr, 51(3): 1432-1442, doi:10.4319/lo. 2006.51.3.1432.

Sarma V V S S, Abe O, Saino T. 2003. Chromatographic separation of nitrogen, argon, and oxygen in dissolved air for determination of triple oxygen isotopes by dual-inlet mass spectrometry. Anal Chem, 75(18): 4913-4917, doi:10.1021/ac034314r.

Sarma V V S S, Abe O, Saino T. 2008. Spatial variations in time-integrated plankton metabolic rates in Sagami Bay using triple oxygen isotopes and O_2: Ar ratios. Limnol Oceanogr, 53(5): 1776-1783, doi:10.4319/lo.2008.53.5.1776.

Seguro I, Marca A D, Painting S J, et al. 2019. High-resolution net and gross biological production during a Celtic Sea spring bloom. Prog Oceanogr, 177: 101885, doi:10.1016/j.pocean.2017.12.003.

Staehr P A, Testa J M, Kemp W M, et al. 2012. The metabolism of aquatic ecosystems: history, applications, and future challenges. Aquat Sci, 74(1): 15-29, doi:10.1007/s00027-011-0199-2.

Stanley R H R, Howard E M. 2013. Quantifying photosynthetic rates of microphytobenthos using the triple isotope composition of dissolved oxygen. Limnol Oceanogr: Methods, 11(7): 360-373, doi:10.4319/lom. 2013.11.360.

Stanley R H R, Kirkpatrick J B, Cassar N, et al. 2010. Net community production and gross primary production rates in the western equatorial Pacific. Glob Biogeochem Cycles, 24(4): GB4001, doi:10.1029/2009GB003651.

Stanley R H R, Sandwith Z O, Williams W J. 2015. Rates of summertime biological productivity in the Beaufort Gyre: a comparison between the low and record-low ice conditions of August 2011 and 2012. J Mar Syst, 147: 29-44, doi:10.1016/j.jmarsys.2014.04.006.

Suggett D, Kraay G, Holligan P, et al. 2001. Assessment of photosynthesis in a spring cyanobacterial bloom by use of a fast repetition rate fluorometer. Limnol Oceanogr, 46(4): 802-810, doi:10.4319/lo.2001. 46.4.0802.

Sweeney C, Gloor E, Jacobson A R, et al. 2007. Constraining global air-sea gas exchange for CO_2 with recent bomb ^{14}C measurements. Glob Biogeochem Cycles, 21(2): GB2015, doi:10.1029/2006GB 002784.

Thiemens M H, Heidenreich J E. 1983. The mass-independent fractionation of oxygen: a novel isotope effect and its possible cosmochemical implications. Science, 219(4588): 1073-1075, doi:10.1126/science.219.4588.1073.

Thiemens M H, Jackson T L, Brenninkmeijer C A M. 1995. Observation of a mass independent oxygen isotopic composition in terrestrial stratospheric CO_2, the link to ozone chemistry, and the possible occurrence in the Martian atmosphere. Geophys Res Lett, 22(3): 255-257, doi:10.1029/94GL02996.

Thiemens M H, Jackson T, Mauersberger K, et al. 1991. Oxygen isotope fractionation in stratospheric CO_2. Geophys Res Lett, 18(4): 669-672, doi:10.1029/91GL00121.

Thiemens M H, Jackson T, Zipf E C, et al. 1995. Carbon dioxide and oxygen isotope anomalies in the mesosphere and stratosphere. Science, 270(5238): 969-972, doi:10.1126/science.270.5238.969.

Thiemens M H, Meagher D. 1984. Cryogenic separation of nitrogen and oxygen in air for determination of isotopic ratios by mass spectrometry. Anal Chem, 56(2): 201-203, doi:10.1021/ac00266a 018.

Tobias C R, Böhlke J K, Harvey J W. 2007. The oxygen-18 isotope approach for measuring aquatic metabolism in high productivity waters. Limnol Oceanogr, 52(4): 1439-1453, doi:10.4319/lo.2007.52.4. 1439.

van der Meer A. 2015. Constraining air-sea equilibrium and biological end-members for marine gross productivity estimates using oxygen triple isotopes. Masters thesis, University of East Anglia.

Watson A J, Upstill-Goddard R C, Liss P S. 1991. Air-sea gas exchange in rough and stormy seas measured by a dual-tracer technique. Nature, 349(6305): 145-147, doi:10.1038/349145a0.

Wurgaft E, Shamir O, Barkan E, et al. 2013. Mixing processes in the deep water of the Gulf of Elat (Aqaba): evidence from measurements and modeling of the triple isotopic composition of dissolved oxygen. Limnol Oceanogr, 58(4): 1373-1386, doi:10. 4319/lo.2013.58.4.1373.

Yakir D, Berry J A, Giles L, et al. 1994. Isotopic heterogeneity of water in transpiring leaves: identification of the component that controls the $\delta^{18}O$ of atmospheric O_2 and CO_2. Plant Cell Environ, 17(1): 73-80, doi:10.1111/j.1365-3040.1994.tb00267.x.

Yung Y L, DeMore W B, Pinto J P. 1991. Isotopic exchange between carbon dioxide and ozone via $O(^1D)$ in the stratosphere. Geophys Res Lett, 18(1): 13-16, doi:10.1029/90GL02478.